Young's modulus of silicon nitride used in scanning force microscope cantilevers

A. Khan, J. Philip, and P. Hess[a)]
Institute of Physical Chemistry, University of Heidelberg, D-69120 Heidelberg, Germany

The Young's modulus and Poisson's ratio of high-quality silicon nitride films with 800 nm thickness, grown on silicon substrates by low-pressure chemical vapor deposition, were determined by measuring the dispersion of laser-induced surface acoustic waves. The Young's modulus was also measured by mechanical tuning of commercially available silicon nitride cantilevers, manufactured from the same material, using the tapping mode of a scanning force microscope. For this experiment, an expression for the oscillation frequencies of two-media beam systems is derived. Both methods yield a Young's modulus of 280–290 GPa for amorphous silicon nitride, which is substantially higher than previously reported ($E = 146$ GPa). For Poisson's ratio, a value of $\nu = 0.20$ was obtained. These values are relevant for the determination of the spring constant of the cantilever and the effective tip–sample stiffness. © *2004 American Institute of Physics.*
[DOI: 10.1063/1.1638886]

I. INTRODUCTION

Silicon nitride is a man-made compound that has been synthesized by different methods. It is considered to be the third hardest material after diamond and cBN. However, the elastic properties, the wear resistance, and the fracture strength of the crystalline and amorphous forms of this material are usually not very well known. In particular, the different crystal phases, such as the two hexagonal structures α- and β-Si_3N_4, and the cubic spinel structure are still under investigation, and our knowledge of their mechanical properties is extremely limited.[1–3] Nevertheless silicon-nitride-based ceramics and amorphous films are presently used in a variety of technological applications.[4–8] These practically applied materials consist of sintered powders or amorphous films deposited by chemical vapor deposition processes in a variety of structures and morphologies with widely unknown mechanical properties.

In scanning force microscopy (SFM), silicon nitride is one of the materials used to produce sharp tips integrated in silicon nitride cantilevers. Due to its low-wear property and higher stiffness, silicon nitride has many advantages compared to silicon, which is also used in this respect. The commercially available cantilevers are prepared by low-pressure chemical vapor deposition (LPCVD) and consist of amorphous material. This leads to a lower rigidity and stiffness than expected for crystalline silicon nitride. Furthermore, the cantilevers are usually coated with thin gold layers ($\sim$60 nm) to improve the reflectivity of the probe laser.

Currently, SFM is the best technique to measure frictional forces on the nanoscale. For a quantitative determination of friction, it is important to know the Young's modulus of the cantilever material and the cantilever dimensions. Various methods are available to determine the normal spring constant of cantilevers.[9–12] The Young's modulus can be determined either from the normal spring constant or from frequency relationships, and vice versa, using an expression given in Ref. 13. To determine the spring constant, the added mass method has been developed.[11] This is a time-consuming approach that is delicate and that can easily damage the tip. Another nondestructive method depends solely on the mass and dimensions of the cantilevers.[12] *Note that all these methods determine the effective normal spring constant or effective Young's modulus of the silicon nitride cantilever, together with the metal coating or gold layer.*

In this article, we present two independent techniques to determine the Young's modulus of LPCVD silicon nitride films: the surface acoustic wave (SAW) method and a mechanical resonance technique using a beam-shaped silicon nitride cantilever. These investigations are performed on commercially available cantilevers and silicon nitride films grown under the same conditions.

II. EXPERIMENTAL PROCEDURE

The general procedure applied to manufacture commercial SFM cantilevers has been described in detail elsewhere.[14] Low-stressed LPCVD films are deposited on the thermal oxide of a Si(100) wafer by using a mixture of dichlorosilane (SiH_2Cl_2) and ammonia (NH_3) in a ratio of 6:1, at a temperature of 750–850 °C, and a pressure of 300 mTorr. For the SAW measurements, a separate silicon nitride film was prepared by the supplier of the cantilevers (Olympus, Japan) using the same procedure employed to produce cantilevers. Therefore, we assume that the silicon nitride samples investigated have similar elastic and mechanical properties. Since the film properties depend on the film thickness, the film had the same thickness of 800 nm as the cantilevers used for the mechanical resonance experiments.

The elastic properties of the silicon nitride film were determined by measuring the dispersion of laser-induced

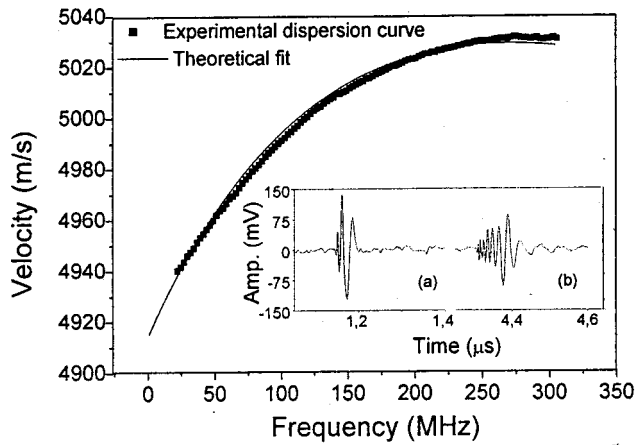[a)]Electronic mail: peter.hess@urz.uni-heidelberg.de

FIG. 1. Experimentally determined dispersion curve and best theoretical fit to extract the elastic constants of the silicon nitride film. Inset: SAW pulses at 8 mm (a) and at 24 mm (b).

SAWs, where the film–substrate system was irradiated with short laser pulses to launch broadband SAW pulses. These surface pulses propagate over a known distance along the surface and are detected with a sensitive broadband poly(vinylidenefluoride) (PVDF)-foil transducer.[15] From the Fourier transformation of the pulse shapes monitored at two different propagation distances, the dispersion of the phase velocity was extracted. To derive the elastic properties, a theoretical model, approximating the film as an isotropic layer but taking into account the anisotropy of the silicon substrate, was applied to fit the theoretical dispersion curves to the measured data.[16]

The commercially available beam-shaped silicon nitride cantilevers (models PSA and PSB from Olympus) were chosen for the resonance measurements. These particular cantilevers were chosen because a theory is available for the resonance vibrations of a bar consisting of one material. To excite the cantilever at its resonances, the tapping mode of the Dimension 3100 Nanoscope IIIa SFM was used. Before the tuning experiment, care was taken that the tip holder was clean and that no dust particles were present between the cantilever and the piezo actuator. Normally, cantilevers have stable and reliable mechanical characteristics with resonance spectra that are simple and free of unexpected vibrational resonances. All tuning experiments were performed under ambient conditions.

III. RESULTS

The inset of Fig. 1 shows two typical SAW pulses measured for the silicon nitride layer on the Si(100) substrate in the ⟨100⟩ direction. They were detected at distances of 8 and 24 mm from the excitation line. The dispersion curve resulting from the Fourier transformation of these two profiles is also presented. Since the phase velocity of SAWs is significantly higher in silicon nitride than in silicon, it increases with frequency in the layered system ("anomalous dispersion").[17] Due to the significant thickness of the silicon nitride film of 800 nm and the acoustic contrast between the two materials, the dispersion curve is nonlinear and two film

properties could be determined. Frequency components up to 300 MHz could be monitored with good signal-to-noise ratio was achieved up to about 250 MHz.

The best theoretical fit to the experimental dispersion curve is also presented in Fig. 1. From this fit, the Young's modulus and Poisson's ratio of the silicon nitride film were extracted by inserting the estimated value of the density and the measured film thickness, as well as the known properties of the silicon substrate.[16] A density of 3.1 g/cm³ was assumed for silicon nitride,[18] which is somewhat lower than the theoretical limit of 3.2 g/cm³.[19] The film thickness of 800 nm was obtained from an optical analysis during film growth. Inserting these two film properties allowed a very good fit of the nonlinear experimental dispersion curve.

The best fit was obtained for a Young's modulus of 289±12 GPa and a Poisson ratio of 0.20±0.05. Generally, the Young's modulus correlates with the density. However, a change in the density by 5% from the value used here leads to significant deviations from the measured dispersion curve. On the other hand, it is important to note that the fit is not very sensitive to changes in Poisson's ratio. This fact leads to the much larger error given for this quantity. While a value of 0.27 can be found in the literature,[20] the lower Poisson's ratio of 0.20 seems to be consistent with the relatively high stiffness of the material investigated.

The values reported in the literature for the Young's modulus of LPCVD silicon nitride vary between 146 and 290 GPa,[9,14,18,21–24] whereas for single-crystal Si_3N_4, a much higher stiffness in the range of 400 GPa is expected.[23] This indicates a considerably lower stiffness of the best amorphous LPCVD films compared to single crystals. This decrease in stiffness can be attributed to the influence of an interfacial transition layer and a lower three-dimensional connectivity in the amorphous material caused by defects, distortions, etc. It should be pointed out that the SAW method leads to mean values of the elastic properties, averaged over the macroscopic propagation distances of the surface wave and the total film thickness.

The second method used to determine the Young's modulus was the mechanical tuning method. The critical issue in choosing between a V-shaped or beam-shaped cantilever has been addressed elsewhere.[25] For the present beam–cantilever system, consisting of two materials, the equation of motion can be described by (see Appendix)

$$\frac{\partial^2 y}{\partial t^2} = -\kappa_{\text{eff}}^2 c_{\text{eff}}^2 \frac{\partial^4 y}{\partial x^4}, \tag{1}$$

and the allowed resonance frequencies are

$$f = \frac{\pi c_{\text{eff}} \kappa_{\text{eff}}}{8L^2}(1.194^2, 2.988^2, 5^2, 7^2, \ldots), \tag{2a}$$

or

$$f_1, 6.27f_1, 17.54f_1, 343.7f_1, \ldots, \tag{2b}$$

where

$$\kappa_{\text{eff}} = \frac{t_1 \kappa_1^2 + \frac{E_2}{E_1} t_2 \kappa_2^2}{t_1 + t_2}, \quad c_{\text{eff}} = \sqrt{\frac{E_1}{\rho_{\text{eff}}}}$$
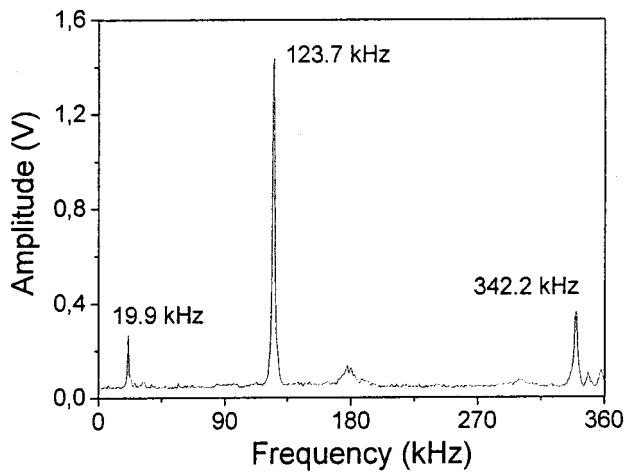
FIG. 2. Mechanically tuned resonance frequencies of an as-delivered, beam-shaped cantilever.
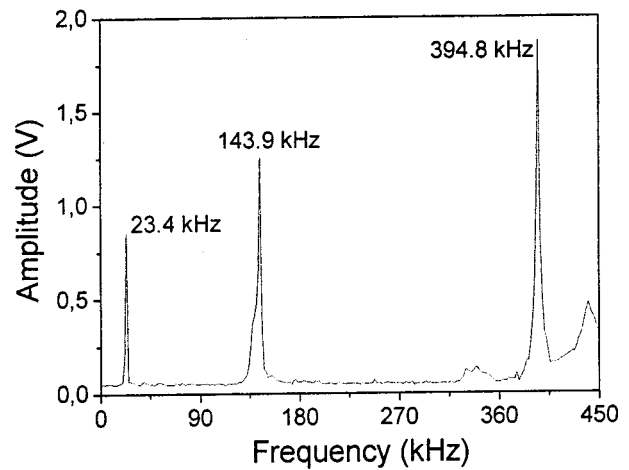

FIG. 3. Mechanically tuned resonance frequencies obtained after complete removal of the original gold coating and redeposition of a known gold film thickness on the probe side of the cantilever.

and the effective density

$$\rho_{\text{eff}} = \frac{\rho_1 t_1 + \rho_2 t_2}{t_1 + t_2},$$

L is the length of the cantilever, κ is the radius of gyration, E is the Young's modulus, c is the longitudinal velocity in the bar, and t is the thickness of the beam.

Equations (1) and (2) are valid only for a beam system in which the thickness of one medium is much larger than the other one and the compliance of the thicker medium is lower than that of the thinner one. As mentioned before, the cantilevers used as SFM probes are covered with a coating for better reflection of the diode laser. In the present case, this coating consists of a 50–70 nm gold film, which is thin compared to the substrate thickness of ~800 nm. Due to its high density of 19.3 g/cm^3, and its high compliance compared to silicon nitride, the thin gold film will mainly contribute weight to the cantilever oscillations, while leaving the mechanical properties of the system approximately the same. For such a beam-shaped silicon nitride cantilever, the weight percentage of the gold film is ~50% of the total weight. Accordingly, such a thin gold film will reduce the resonance frequency by approximately ~33%.

Figure 2 shows the mechanically-tuned resonances of the beam-shaped cantilever used as delivered. Figure 3 presents these resonances of the same cantilever after complete removal of the original gold film deposited by the manufacturer and redeposition of a gold film of 50 nm thickness only on the back side of the cantilever. A comparison indicates that the first resonance frequency f_1 increases from 19.9 to 23.46 kHz. This indicates that the manufacturer provides cantilevers with a coating on both sides of the cantilever. Obviously, the experimentally measured frequencies are in good agreement with those calculated in both cases before and after modification of the cantilever (see Table I).

For the 800-nm-thick silicon nitride beam with 201 μm length and a 50 nm gold film on one side, the resulting Young's modulus was 280 ± 30 GPa. For the analysis, we applied the simplified version of a two-media beam system and assumed that the velocities in the two combined media

were same. The cantilever dimensions were measured by scanning electron microscopy. Obviously, the resonance method yields a Young's modulus very close to the SAW result of 289 GPa, but much higher than the value provided by the manufacturer (146 ± 20 GPa).[18] Interestingly, the frequencies provided by the manufacturer agreed within experimental error with those measured here. The Young's moduli were derived from the experimental frequencies, however, the influence of the gold film was ignored. For V-shaped silicon nitride cantilevers, a Young's modulus of 180 ± 20 GPa has been reported obtained by the cantilever deflection method.[9] In this case, the analysis is not as straightforward as for beams.

IV. DISCUSSION

The Young's modulus of amorphous silicon nitride, used as cantilever material, was determined by SAW dispersion and mechanical resonance experiments. Within the large range of stiffnesses reported in the literature for amorphous silicon nitride, the SAW and mechanical resonance values of $E = 289$ and 280 GPa, respectively, represents the upper limit and are about twice the value of $E = 146$ GPa provided by the manufacturer of such cantilevers (Olympus, Japan). This discrepancy is due mainly to an oversimplified analysis of the previous measurements. On the other hand, a Poisson ratio of 0.20 is considerably smaller than the literature value of 0.27. Unfortunately, a comparison with the optimal single-

TABLE I. Comparison of measured frequencies for the cantilever before and after modification with the theoretically estimated frequencies.

Theoretically estimated frequencies (kHz)	Frequencies measured for new cantilever (kHz)	Frequencies measured after removal and redeposition of gold film (kHz)
f_1	19.9 (f_1)	23.4 (f_1)
6.27 f_1	123.7 (6.22 f_1)	143.9 (6.15 f_1)
17.54 f_1	342.2 (17.2 f_1)	394.8 (16.9 f_1)

crystal properties of Si_3N_4, signifying the ultimate limit for this material, can not be performed since these elastic constants are missing.

The present Young's modulus indicates that silicon nitride tips are much stiffer than could be expected from the former value. Accordingly the hardness should also be higher and the wear lower than suggested by the previous results. This qualitative conclusion may be drawn despite the fact that the mechanical behavior of the tip end in an SFM measurement is widely unknown. The present elastic constants of amorphous silicon nitride are superior to those of crystalline silicon, with a mean Young's modulus of about 160 GPa and a Poisson ratio of 0.22 (Ref. 26) and those typically used for silicon cantilevers of $E = 129$ GPa and $\nu = 0.28$.[27] This is consistent with practical experience in SFM measurements.

However, it is important to keep in mind that both silicon and silicon nitride tips are covered with an ultrathin native oxide layer that influences microscopic interaction forces and may also affect the mechanical contact behavior. This oxide layer introduces additional uncertainties into the determination of the effective elastic tip–sample modulus, depending on the reduced Young's modulus of the contact. This latter quantity is determined by the Young's moduli and Poisson's ratios of the tip and the sample. The values known for amorphous silicon dioxide ($E = 70$ GPa, $\nu = 0.27$) point to a decrease of the effective Young's modulus and increase of the effective Poisson's ratio of the tip by the native oxide layer.

ACKNOWLEDGMENTS

APPENDIX

Consider a straight bar of length L with the thickness t, having a uniform cross section S with a bilateral symmetry. The x coordinate measures positions along the bar, and the y coordinate the transverse displacement. When the bar is bent as shown in Fig. 4, the upper part will be stretched and lower part will be compressed while having the neutral axis somewhere between the upper and the lower part. For a bar of one medium fixed at one end and vibrating transversely, the allowed frequencies are:[28]

$$f = \frac{\pi c \kappa}{8L^2}(1.194^2, 2.988^2, 5^2, 7^2, \ldots), \quad (A1)$$

where

$$c = \sqrt{\frac{E}{\rho}} \quad \text{and} \quad \kappa = \frac{t}{\sqrt{12}}.$$

Consider the segment of the bar of length l_x and assume that the bending of the bar is measured by the radius of
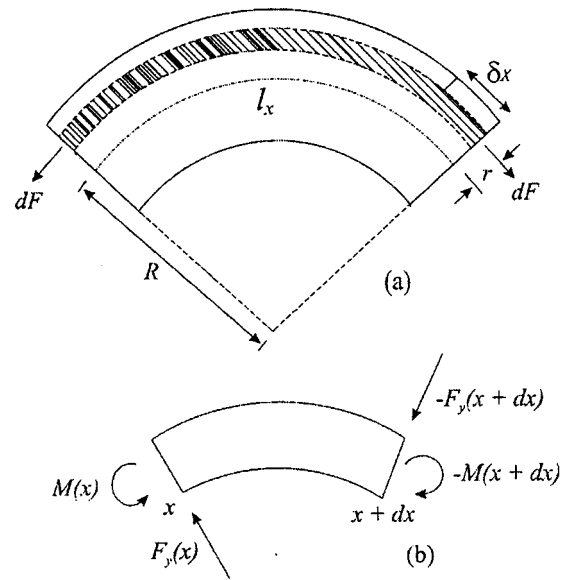

FIG. 4. Bending strains and stresses (a) and bending moments and shear forces (b) in one medium.

curvature R of the neutral axis. Let δx be the increment due to the bending of the filament of the bar located at a distance r from the neutral axis.

Now, we consider a two-media system with Young's moduli E_1 and E_2, densities ρ_1 and ρ_2, and uniform cross sections S_1 and S_2 (see Fig. 5). For such a system, the following equations can be derived with the help of Ref. 28.

The longitudinal force dF in each medium can be written as

$$dF_1 = -E_1 dS_1 \frac{\delta x_1}{l_x}; \quad dF_2 = -E_2 dS_2 \frac{\delta x_2}{l_x}, \quad (A2)$$

and from the geometry we obtain

$$\frac{l_x + \delta x_1}{R + r_1} = \frac{l_x}{R} = \frac{l_x + \delta x_2}{R + r_2}, \quad (A3a)$$

and

$$\frac{\delta x_1}{l_x} = \frac{r_1}{R}; \frac{\delta x_2}{l_x} = \frac{r_2}{R}. \quad (A3b)$$

From Eqs. (A2) and (A3),

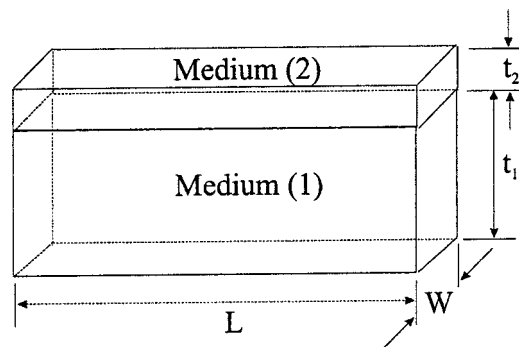FIG. 5. Two-media system with $t_1 \gg t_2$.

$$dF_1 = -E_1 dS_1 \frac{r_1}{l_x}; \quad dF_2 = -E_2 dS_2 \frac{r_2}{l_x}. \tag{A4}$$

The total longitudinal force $F = \int dF$ will be zero. Positive forces below the neutral axis will be cancelled by the negative forces above the neutral axis. However, a resulting bending moment M will be present in the system, which can be written as

$$\begin{aligned}
M &= \int r_1 dF_1 + \int r_2 dF_2 \\
&= -\frac{E_1}{R} \int r_1^2 dS_1 - \frac{E_2}{R} \int r_2^2 dS_2 \\
&\approx -\left(\frac{E_1 S_1 \kappa_1^2}{R} + \frac{E_2 S_2 \kappa_2^2}{R} \right) \\
&= -(E_1 S_1 \kappa_1^2 + E_2 S_2 \kappa_2^2) \frac{\partial^2 y}{\partial x^2}, \tag{A5}
\end{aligned}$$

$$\left(\text{for small displacements, } R \approx \frac{1}{\partial^2 y / \partial x^2} \right),$$

where

$$\kappa_1^2 = \frac{\int r_1^2 dS_1}{S_1} \quad \text{and} \quad \kappa_2^2 = \frac{\int r_2^2 dS_2}{S_2}$$

can be considered as the radii of gyration of the cross-sectional areas S_1 and S_2, respectively.

From the Fig. 4(b), a relation between the bending moment M and shear force F_y can be written as

$$M(x) - M(x+dx) = F_y(x+dx)dx. \tag{A6}$$

For a segment of small length dx, $M(x+dx)$ and $F_y(x+dx)$ can be expanded to Taylor expansions about x, yielding

$$F_y = -\frac{\partial M}{\partial x} = (E_1 S_1 \kappa_1^2 + E_2 S_2 \kappa_2^2) \frac{\partial^3 y}{\partial x^3}. \tag{A7}$$

Again, from the Fig. 4(b), the net upward force dF_y acting on the segment d_x can be given by

$$\begin{aligned}
dF_y &= F_y(x) - F_y(x+dx) \\
&= \frac{\partial F_y}{\partial x} dx = -(E_1 S_1 \kappa_1^2 + E_2 S_2 \kappa_2^2) \frac{\partial^4 y}{\partial x^4}. \tag{A8}
\end{aligned}$$

This will give an upward acceleration and, since the mass of the segment is $\rho_i S_i dx$, the equation of motion of the two-media system can be written as

$$(\rho_1 S_1 + \rho_2 S_2) dx \frac{\partial^2 y}{\partial t^2} = -(E_1 S_1 \kappa_1^2 + E_2 S_2 \kappa_2^2) \frac{\partial^4 y}{\partial x^4} dx, \tag{A9a}$$

or

$$\frac{\partial^2 y}{\partial t^2} = \frac{(E_1 S_1 \kappa_1^2 + E_2 S_2 \kappa_2^2)}{(\rho_1 S_1 + \rho_2 S_2)} \frac{\partial^4 y}{\partial x^4}, \tag{A9b}$$

dividing the numerator and denominator by $S_1 + S_2$ and rearranging the equation

$$\frac{\partial^2 y}{\partial t^2} = -\kappa_{\text{eff}}^2 c_{\text{eff}}^2 \frac{\partial^4 y}{\partial x^4}, \tag{A9c}$$

where

$$\kappa_{\text{eff}} = \frac{S_1 \kappa_1^2 + \frac{E_2}{E_1} S_2 \kappa_2^2}{S_1 + S_2}, \quad c_{\text{eff}} = \sqrt{\frac{E_1}{\rho_{\text{eff}}}}$$

and

$$\rho_{\text{eff}} = \frac{\rho_1 S_1 + \rho_2 S_2}{S_1 + S_2}.$$

For the length $L_1 = L_2$ and width $W_1 = W_2$,

$$k_{\text{eff}} = \frac{t_1 \kappa_1^2 + \frac{E_2}{E_1} t_2 \kappa_2^2}{t_1 + t_2}, \quad c_{\text{eff}} = \sqrt{\frac{E_1}{\rho_{\text{eff}}}},$$

and

$$\rho_{\text{eff}} = \frac{\rho_1 t_1 + \rho_2 t_2}{t_1 + t_2},$$

and the allowed resonance frequencies are given in the text [Eq. 2(a)].

[1] A. Zerr, G. Miehe, G. Serghio, M. Schwarz, E. Kroke, R. Riedel, H. Fueß, P. Kroll, and R. Boehler, Nature (London) **400**, 340 (1999).
[2] R. Vogelgesang, M. Grimsditch, and J. S. Wallace, Appl. Phys. Lett. **76**, 982 (2000).
[3] G. A. Swift, E. Üstündag, B. Clausen, M. A. M. Bourke, and H. Lin, Appl. Phys. Lett. **82**, 1039 (2003).
[4] T. Aoyama, H. Tashiro, and K. Suzuki, J. Electrochem. Soc. **146**, 1879 (1999).
[5] K. A. Ellis and R. A. Buhrman, Appl. Phys. Lett. **74**, 967 (1999).
[6] D. Mathiot, A. Straboni, E. Andre, and P. Debenest, J. Appl. Phys. **73**, 8215 (1993).
[7] S. A. Cambell, *The Science and Engineering of Microelectronic Fabrication* (Oxford University Press, New York, 1996), Chap. 15, p. 390.
[8] S. Leclerc, A. Lecours, M. Caron, E. Richard, G. Tucrotte, and J. F. Currie, J. Vac. Sci. Technol. A **16**, 881 (1998).
[9] E. Liu, B. Blanpain, and J. P. Celis, Wear **192**, 141 (1996).
[10] N. Maeda and T. J. Senden, Langmuir **16**, 9282 (2000).
[11] J. P. Clevland, S. Manne, D. Bocek, and P. K. Hansma, Rev. Sci. Instrum. **64**, 403 (1993).
[12] J. E. Sader, I. Larson, P. Mulvaney, and L. R. White, Rev. Sci. Instrum. **66**, 3789 (1995).
[13] For the beam-shaped cantilevers, the frequency expression is given by $f = 0.178 \pi ck/L^2$ (see Appendix) and normal spring constant by $k = Et^3 w/4(L - \Delta L)$ (see Ref. 25).
[14] T. R. Albrecht, S. Akamine, T. E. Carver, and C. F. Quate, J. Vac. Sci. Technol. A **8**, 3386 (1990).
[15] H. Coufal, R. Grygier, P. Hess, and A. Neubrand, J. Acoust. Soc. Am. **92**, 2980 (1992).
[16] G. Lehmann, P. Hess, S. Weissmantel, G. Reisse, P. Scheible, and A. Lunk, Appl. Phys. A: Mater. Sci. Process. **74**, 41 (2002).
[17] A. Lomonosov, A. P. Mayer and P. Hess, in *Modern Acoustical Techniques for the Measurement of Mechanical Properties*, edited by M. Levy, H. E. Bass, and R. Stern (Academic, Boston, 2001) Vol. 9, pp. 65–134.
[18] K. E. Petersen, Proc. IEEE **70**, 420 (1982).
[19] *Powder Diffraction File-2 Database* (JCPDS Int. Centre for Diffraction Data, Newton Square, PA, 1996).
[20] C. T. Lynch, *CRC Materials Science and Engineering Handbook* (CRC Press, Boca Raton, FL, 1989) p. 321.
[21] C. J. Drumond and T. J. Senden, Meas. Sci. Technol. **189−190**, 107 (1995).
[22] J. A. Taylor, J. Vac. Sci. Technol. A **9**, 2464 (1991).
[23] P. Walsh, A. Omeltchenko, R. K. Kalia, A. Nakano, P. Vashishta, and S. Saini, Appl. Phys. Lett. **82**, 118 (2003).

[24] O. Tabata, K. Kawahata, S. Sugiyama, and I. Igarashi, Sens. Actuators **20**, 135 (1989).

[25] J. E. Sader, Rev. Sci. Instrum. **74**, 2438 (2003).

[26] R. Kuschnereit, H. Fath, A. A. Kolomenskii, M. Szabadi, and P. Hess, Appl. Phys. A: Mater. Sci. Process. **61**, 269 (1995).

[27] R. W. Stark, G. Schitter, and A. Stemmer, Phys. Rev. B **68**, 085401 (2003).

[28] L. E. Kinsler, A. R. Frey, A. B. Coppens, and J. V. Sanders, *Fundamentals of Acoustics*, 3rd ed. (Wiley, New York, 1982) Chap. 3, p. 68.